JOURNAL OF SYNCHROTRON RADIATION

Volume 28 (2021)

Supporting information for article:

Development of a novel microfluidic device to study metal geochemistry *in situ* using X-ray fluorescence microprobe spectroscopy

Michael A. Chen and Benjamin D. Kocar

S1. Additional information about materials and methods

S1.1. Re-use of microfluidic devices

Methods for recycling or reusing the etched silicon micromodels were also investigated to help mitigate the time and cost associated with creating new micromodels. Used micromodels could sometimes be recycled by removal of the thin glass and Nanoports, followed by cleaning using an appropriate solution. First, a complete device was disconnected from flow lines, and submerged in clean acetone for at least 3 hours. This process weakened the epoxy and UV glue sufficiently to release the nanoport fittings and thin glass coverslip. A razor blade was sometimes used to gently pry the cover slip and nanoports from the weakened adhesive, if necessary, followed with additional soaking in acetone for 3 or more hours to remove residual adhesive. If the glass would not release after these steps, then the device was washed in acetone and isopropanol (to remove any acetone-organic) residues, heated to 650 °C in a muffle furnace, and then immediately allowed to cool to room temperature while remaining in the furnace, which burned off any residual epoxy. Any remaining glass was then removed, and the pore network cleaned, typically by immersion in piranha solution (1 part H_2O_2:3 parts concentrated H_2SO_4) for 15 min. After cleaning, the device was re-fired at 1000 °C to restore any removed SiO_2 coatings and to remove any remaining organic residues. Note that care was taken to ensure complete removal of the coverslips from the silicon devices before heat treatment, as prolonged heating at elevated temperatures (> 650 °C) led to incomplete bonding of any remaining glass directly to the silicon device.

S1.2. Background solution preparation and details

A BSS was used as the background for all solutions infused into microfluidic devices, except for those containing Fe(II), as Fe(III) rapidly precipitated out of solution when Fe(II) was added to the BSS. The composition of this BSS is given in table S1. Large batches (2 L) of BSS were mixed and titrated to pH 7.10+/- 0.05 using either 0.4 M NaOH or 0.12 M HCl. This solution composition was adapted from a previous work, and is taken to be a representative groundwater condition (Kocar *et al.*, 2006).

Table S1 Basal salts solution used in microfluidic experiments and adapted from previous work (Kocar *et al.*, 2006). Ingredients were added in the order listed in the table, allowing for complete dissolution before adding the next ingredient. After all ingredients were added, the solution was titrated to pH 7.1 using either 0.4 M NaOH or 0.12 M HCl, as required.

Component	Concentration (mM)
KCl	2.7
$MgSO_4 \cdot 7\ H_2O$	0.6
NaCl	7.9
NH_4Cl	0.0002
$CaCl_2 \cdot H_2O$	0.4
$NaHCO_3$	3.7
NaPIPES	50
Wolfe's mineral solution (ATCC)	0.1 mL/L

S1.3. Photolithography mask preparation

The masks used in photolithography were printed on laminate, containing a bitmap image that had the desired microfluidic device design. These were created in Adobe Illustrator, which allowed for fine scale manipulation of the required shapes needed to define the microfluidic device and pore regions. This also allowed for programmatic randomization of the pore features found in middle region of the parallel flow design (figure 1). This was performed on each pore post using the parameters defined in table S2.

Table S2 Randomization parameters for microfluidic device applied using Adobe Illustrator (version 22.1). The distribution for values is even from none to the set value, thus these set values indicate the maximal value of the parameter.

Parameter	Set Value
Horizontal displacement	0.05 mm
Vertical displacement	0.2 mm
Horizontal scaling	120%
Vertical scaling	75%
Rotation	90°

S2. Additional results

S2.1. Background spectra of the glass window

The 30 μm glass used to seal devices was found to contain appreciable amounts of other elements that may interfere with the analyses performed here. An XRF spectrum up to 11 keV was collected on a clean glass sample that was not attached to a microfluidic device, given in figure S1. The contributing elements are marked directly in the figure. There are major measured signals from fluorescence lines of Ba and Fe, which would interfere with analyses of elements within 4 keV to 7.5 keV. In the case of Fe analysis here, Fe solid concentrations were high enough to observe Fe solids beyond this interference (figure 3). This interference did, however, prevent the application of multi-energy mapping to Fe as the fitted signals attempted to include the speciation of Fe in the glass.

Figure S1 Background spectrum of the thin glass used to seal microfluidic devices. Relevant elemental peaks are labelled.

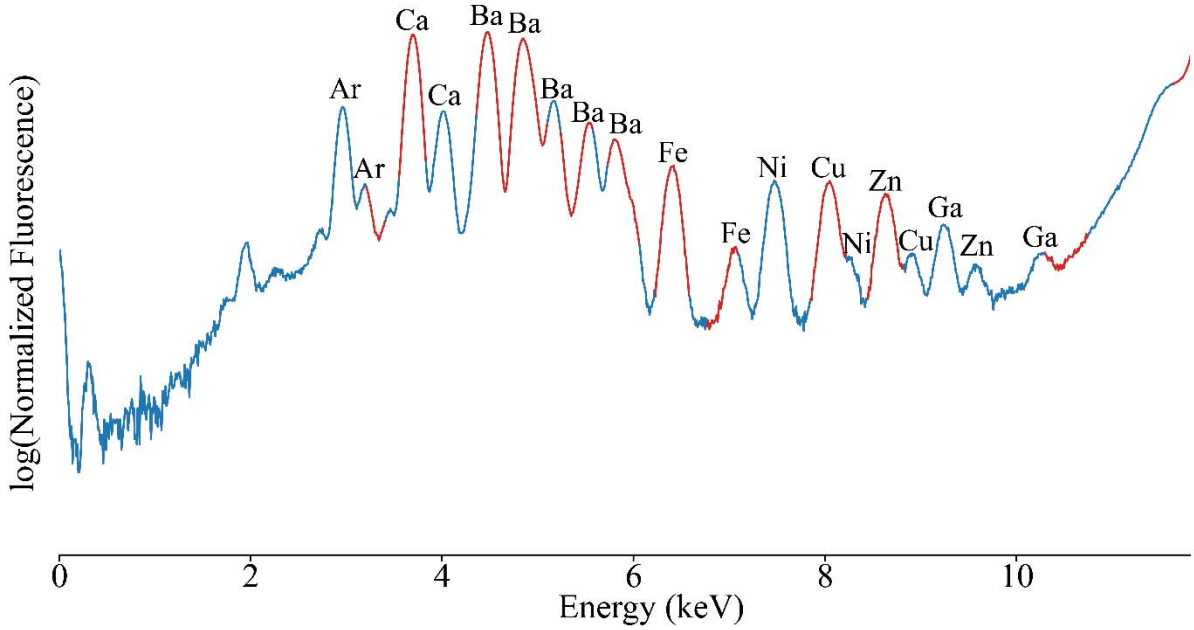

S2.2. Time series maps of parallel flow devices over time

Parallel flow devices were mapped regularly at 14 keV throughout the infusion of the different solutions to track the evolution of spatial patterns of As and Br at each reaction stage. The device designs led to solutions reaching the entirety of the pore regions, which differs from the diverging flow devices in which Br never reached the side opposite of its injection, regardless of how long the devices were run. Maps of As, Br, and Fe at each major reaction stage, that is, after complete introduction of As, complete flushing of that As with BSS, and introduction of S are given in figure S2. A stage was considered “complete” when Br was observed to have a stable spatial pattern. When

Br was introduced, it would eventually permeate the entire porous region, while when being flushed, would be completely removed.

Figure S2 Snapshots of Br, As, and Fe distributions in a single parallel flow device throughout the specified solution sequence. Maps taken during As infusion and S infusion were at 12 μm step size and during BSS flushing, 40 μm.

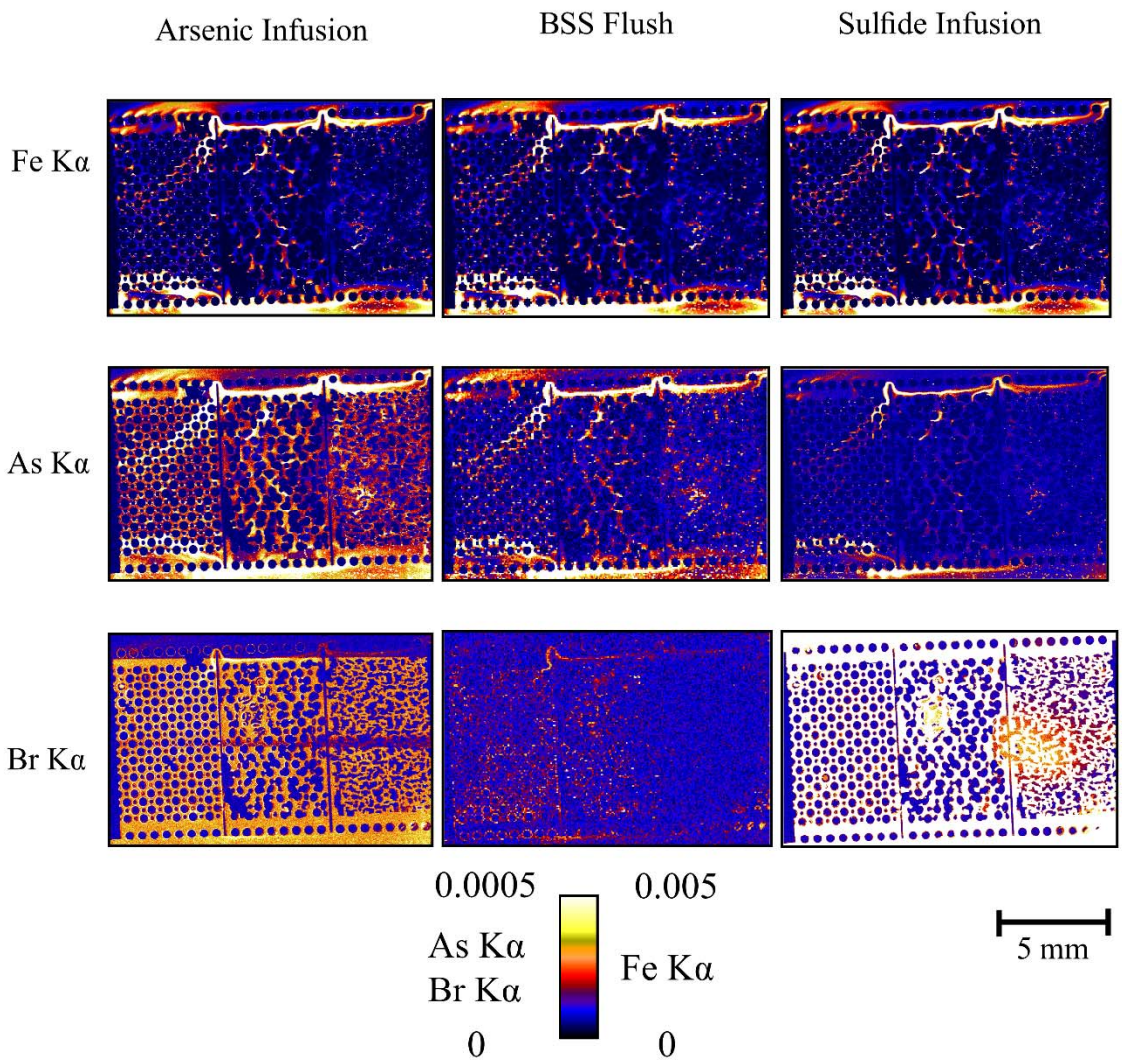

S2.3. Additional XAS results

The averaged XAS spectra used for LCF fitting presented in table 1 and 2 are given, alongside the appropriate XAS standards, in figure S3 (As) and S4 (Fe). The points where these spectra were taken are given in figure S5, which places the points on the relevant XRF fluorescence map. Multiple spectra were taken to average out noise, though in some cases, this was not possible for As, owing to beam damage which manifested as a transformation of the As signal over successive XAS measurements. A beam damage study showing the shifting As spectra is given in figure S6,

which was taken after a parallel flow device had been infused with As. The specific As form that has formed cannot be positively identified using the samples used here, nor do they match with previously measured As spectra (Mogren *et al.*, 2013; Smith *et al.*, 2005). Each scan required 4 minutes of direct beam expsoure, with the transition to the unknown peak occuring after the 2nd scan (8 minutes of exposure time). It is unlikely that the prior mapping would have intitated this transformation because the observed transition required more than 8 minutes of direct exposure, which is much less than the beam exposure by mapping (where each point is exposed, at most, for 200 ms/point/map). Indeed, the XAS spectra presented in figure S4 were taken both before and after this beam damage study, and showed none of the characteristics (i.e. the unknown peak) of that found during the beam damage study. Thus it is unlikely that mapping would interfere of collection of XANES spectra, nor vice versa, as the beam size used to collect the XANES spectra was very small compared to the mapped area (5-45 μm).

Figure S3 Fe XANES spectra with the fitted Fe standards. All spectra were collected after reaction with sulfide, in a device that was analysed after the full experimental sequence.

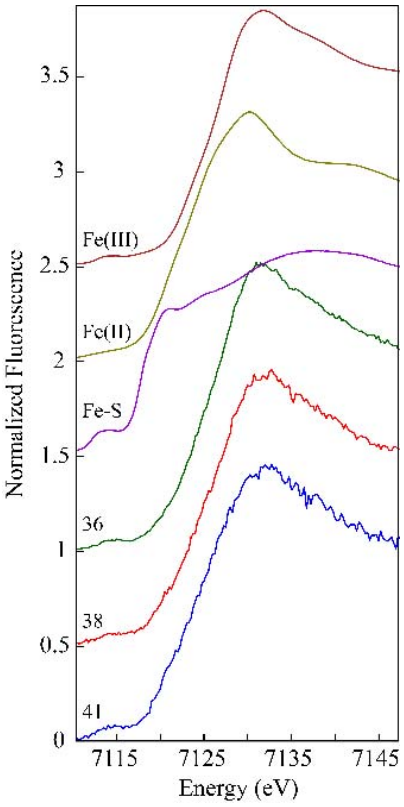

Figure S4 As XANES points and the relevant standards. Numbers indicate the point measured, while the codes indicate at what point in the injection sequence the spectra were taken. As stands for during the As injection, while S indicates it was taken during the S injection.

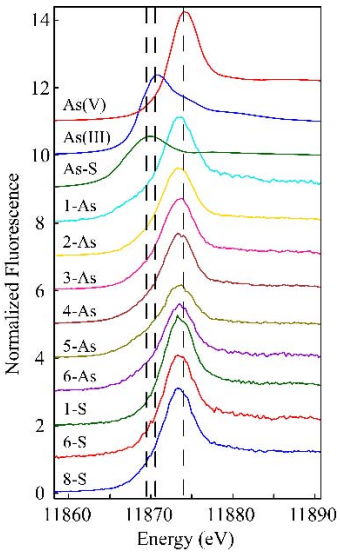

Figure S5 Location of referenced XANES points, accompanied by the relevant XRF map. a) Fe XANES points and b) As XANES points. Both XRF map values are elemental counts normalized to incident beam energy. Note that different devices were used to collect the maps in a) and b), resulting in the differences in observed elemental distributions. Note that XANES for Fe were taken in a different device than for As, thus the distributions will not align.

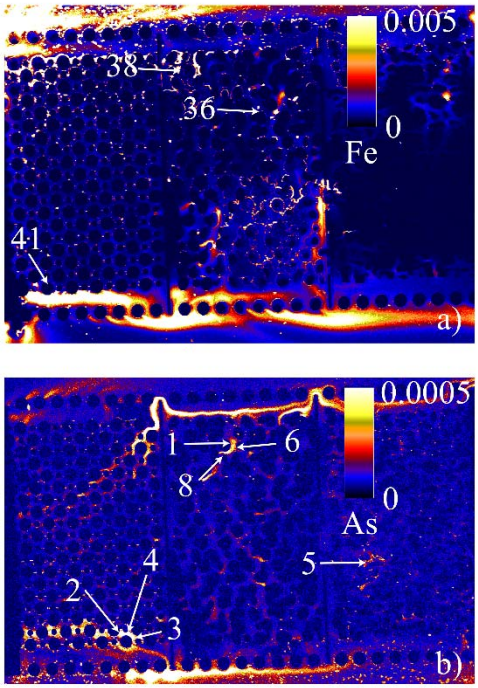

Figure S6 Evidence for the impact of the beam on As speciation after multiple subsequent scans. Each scan required approximately 4 minutes of time. The initial scans show a peak near 11874 eV, suggesting the predominant species is As(V), but the following scans have a peak around 11867 eV, which does not match any of the standards considered here.

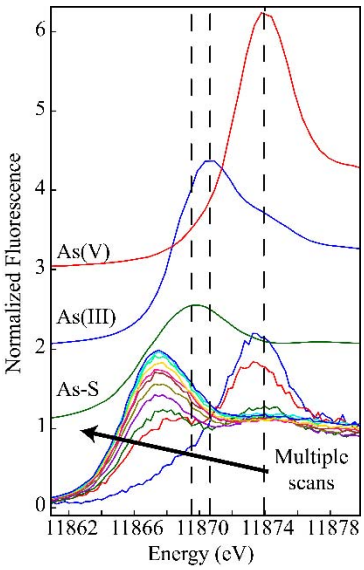

S2.4. Additional ME Mapping Results

Additional regions were selected for ME mapping to look for spatial variations in the distribution of As species as a function of the infused solutions, and are presented in figure S7. A contextual figure showing Fe counts for the same areas and time points is given in figure S8. Trends in As speciation change depending on the location, but as indicated by Br tracer presence throughout the device (figure S2), it is not immediately clear why these difference emerge. In all regions, however, no As-S species are found, as confirmed by the XAS results.

Figure S7 Results of ME mapping for three different areas of the parallel flow device. Randomized pores refer to the randomized pore space in the middle of the device, regular pores the repeating posts, and sandstone the region derived from a natural sandstone.

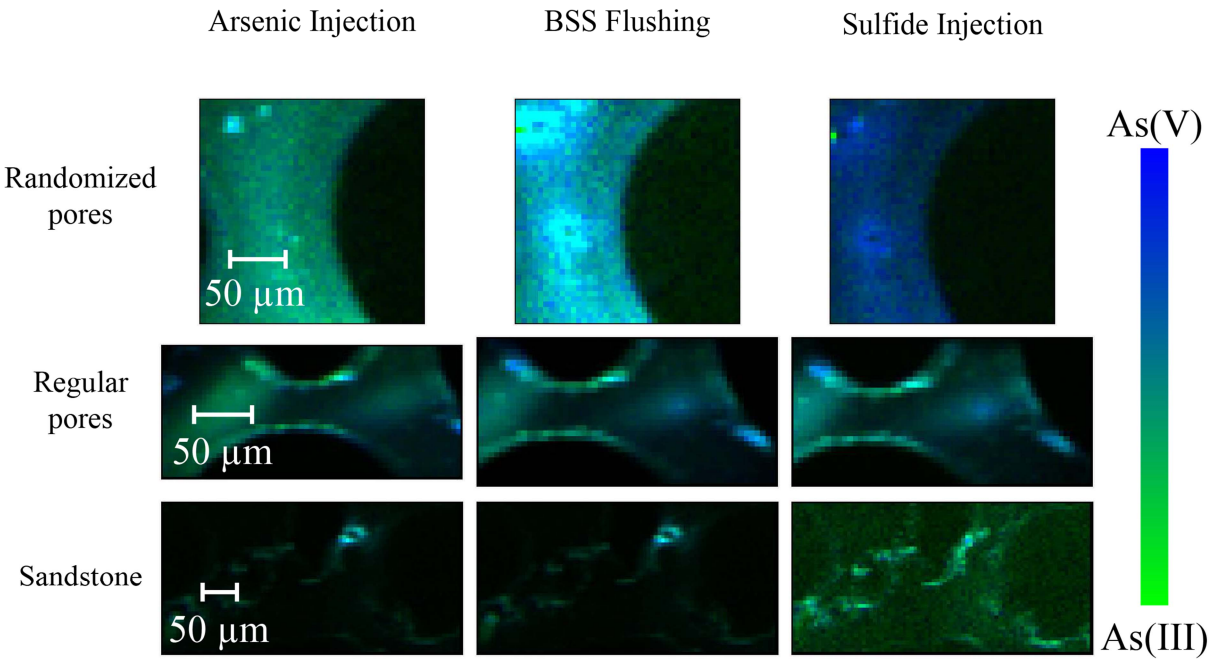

Figure S8 Fe Kα XRF maps corresponding to the areas and time points used for ME mapping indicated in Figure S7.